

Supporting information

Table of Contents

MW-assisted hydrothermal synthesis of Ir-based catalysts	3
Powder-XRD (P-XRD)	4
SEM of MW-produced Ir-compounds	5
STEM-imaging	6
Thermogravimetric analysis (TGA) and Differential scanning calorimetry (DSC)	7
Temperature programmed reduction (TPR)	9
Quantification of the samples composition and average Ir-oxidation state	9
OER-activity evaluated from linear sweep voltammetry (LSV).....	11
OER-stability evaluated from chronopotentiometry (CP)	12

Table S1. Summary of the main synthesis parameters such as KOH:Ir and T_{syn} as well as synthesis yield, K- and Cl-contents and specific surface area (S_{BET}) of the produced compounds./ H_2 -uptake at room temperature (RT) and consumption during TPR as well as the resulting average oxidation state of iridium in the samples related to the non-metallic phase

KOH:Ir	Synthesis yield (%)	K:Ir (10^{-3})	Cl:Ir (10^{-3})	S_{BET} ($\text{m}^2 \text{g}^{-1}$)	x_{m,H_2O}^{φ}	x_{m,H_2O}^{χ}	IrO _x (OH) _y		$n_{H_2} \cdot n_{Ir}^{-1}$ @ RT	$n_{H_2} \cdot n_{Ir}^{-1}$ TPR	Ir ⁰ -content (mol.%)	Average Ir-oxidation state (oxidic phase)	Internal reference number
							x	y					
1:1	51	2.5±0.12	433	217	2.7	6.0	0.56	1.68	0.05	1.39	0	3.2	21009
4:1	97	3.9±0.17	299	165	2.6	7.0	0.54	1.94	0.36	1.33	0	3.3	21404
5:1	99	18.4±0.26	0	104	1.9	6.7	0.86	1.79	0.53	1.22	0	3.5	21011
7:1	100	91±0.52	0	56	1.9	3.6	1.17	0.93	0.65	0.98	13.2	3.8	21130
10:1	99	112±0.67	0	175	2.6	2.5	1.21	0.66	0.63	0.91	14.6	3.6	21013
50:1	72	92±0.52	0	7	1.7	2.3	1.15	0.58	0.24	1.20	23.6	3.8	21015
100:1	35	36±0.34	0	16	1.2	1.05	n.d.	n.d.	n.d.	n.d.	n.d.	n.d.	21017
SA-IrO ₂	-	0	0	4	0.1	0	2	0	0	2.04	0	4.1	20288
AA-IrO _x	-	0	0	33	0.9	5.1	1.09	1.34	0.59	1.21	2.4	3.6	20233

The synthesis yield results from the ratio of the obtained sample mass and the theoretical mass based on the sample composition obtained for each KOH:Ir ratio according to XRF, TGMS and TPR.

MW-assisted hydrothermal synthesis of Ir-based catalysts

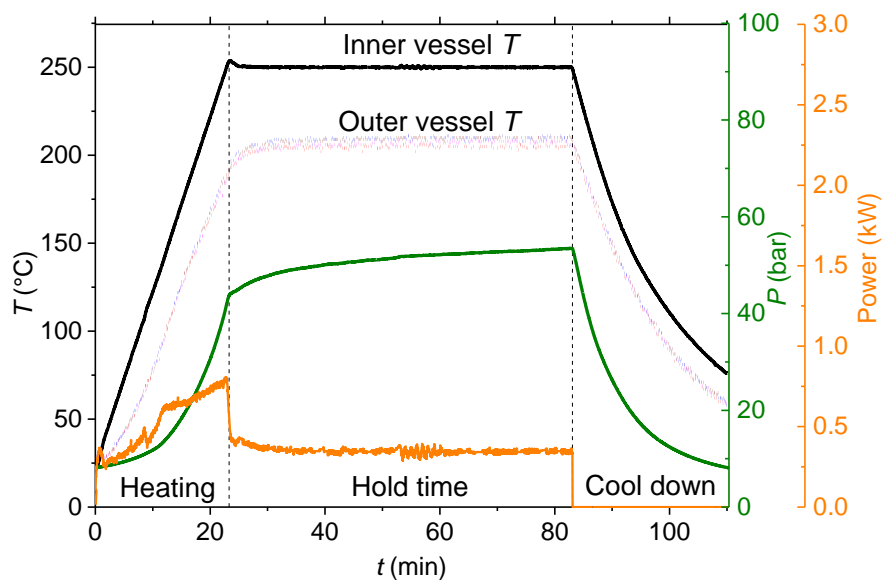


Figure S1. Typical vessel synthesis parameters monitored during the hydrothermal synthesis of Ir-based catalyst for a KOH:Ir=5:1 at 250°C, 1h. The homogeneity of temperatures (T) in the four vessels was verified via IR-measurements of the outer-wall temperature of the four vessels (colored dotted lines), the inner temperature of one vessel was measured using a plunging probe (full black line). The inner vessel pressure (P , green line) and required MW-power (orange line) are also indicated.

Powder-XRD (P-XRD)

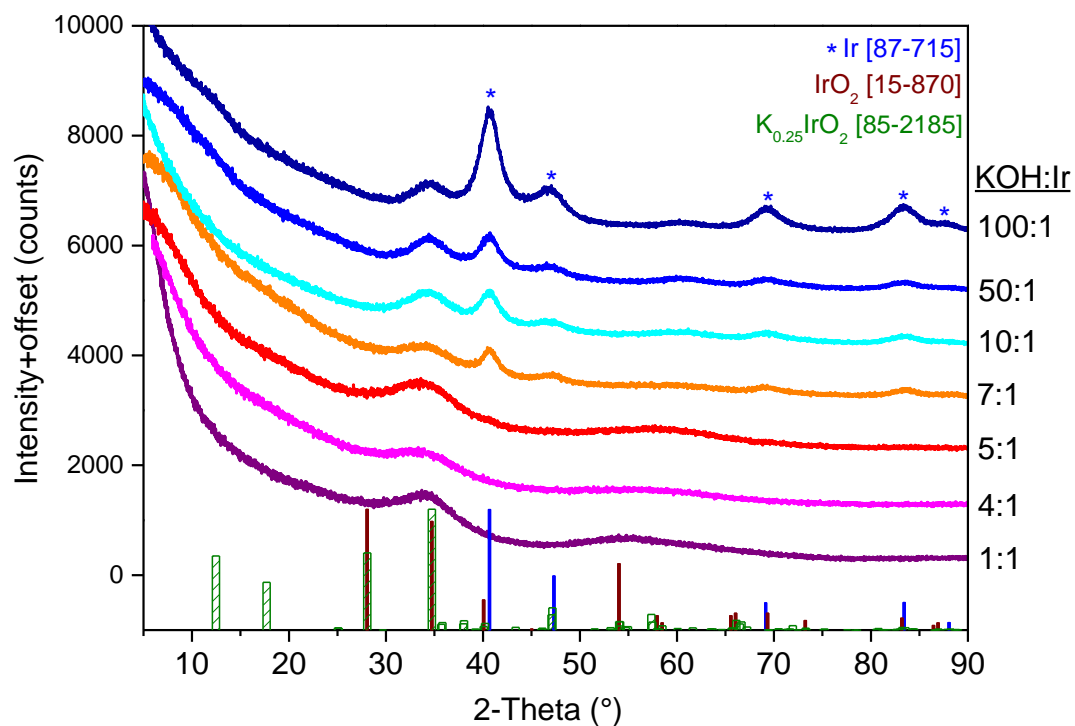


Figure S2. P-XRD patterns of the MW-produced Ir-compounds synthesized for various KOH:Ir-ratios. Reference patterns are shown for crystalline IrO₂ (red bars, PDF [15-870]), K_{0.25}IrO₂ (green bars, PDF [852185]) and Ir⁰ (blue bars and stars, PDF [87-715]).

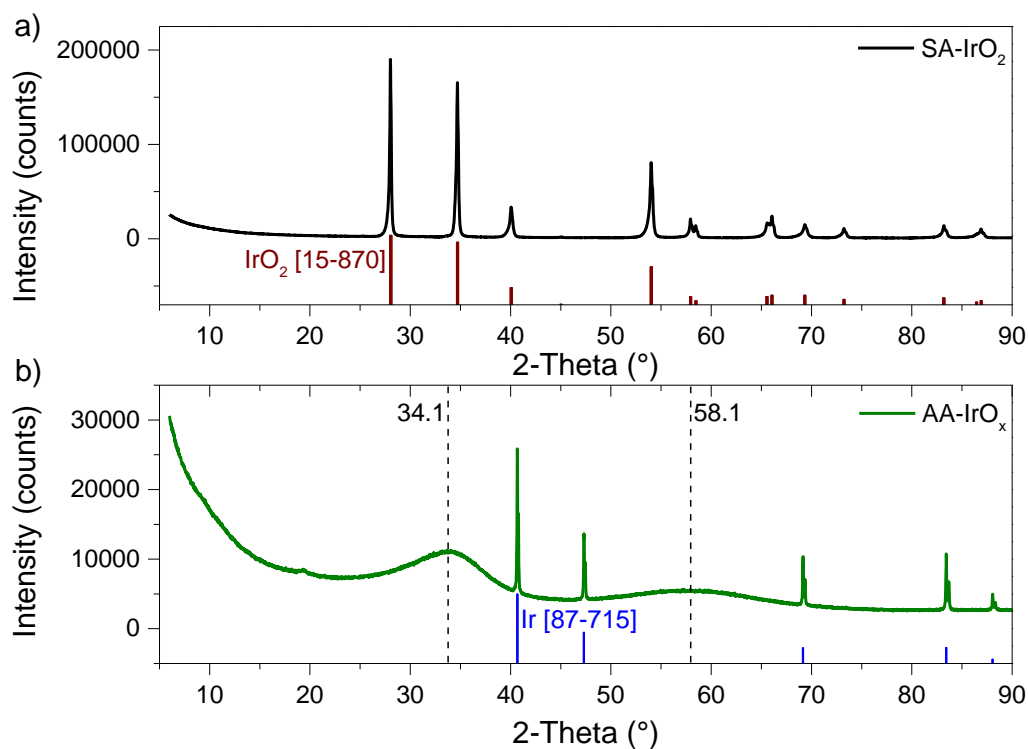


Figure S3. P-XRD patterns of reference compounds (a) SA-IrO₂ (a) and (b) AA-IrO_x. Reference patterns are shown for crystalline IrO₂ (red bars, PDF [15-870]) and Ir⁰ (blue bars and stars, PDF [87-715]).

SEM of MW-produced Ir-compounds

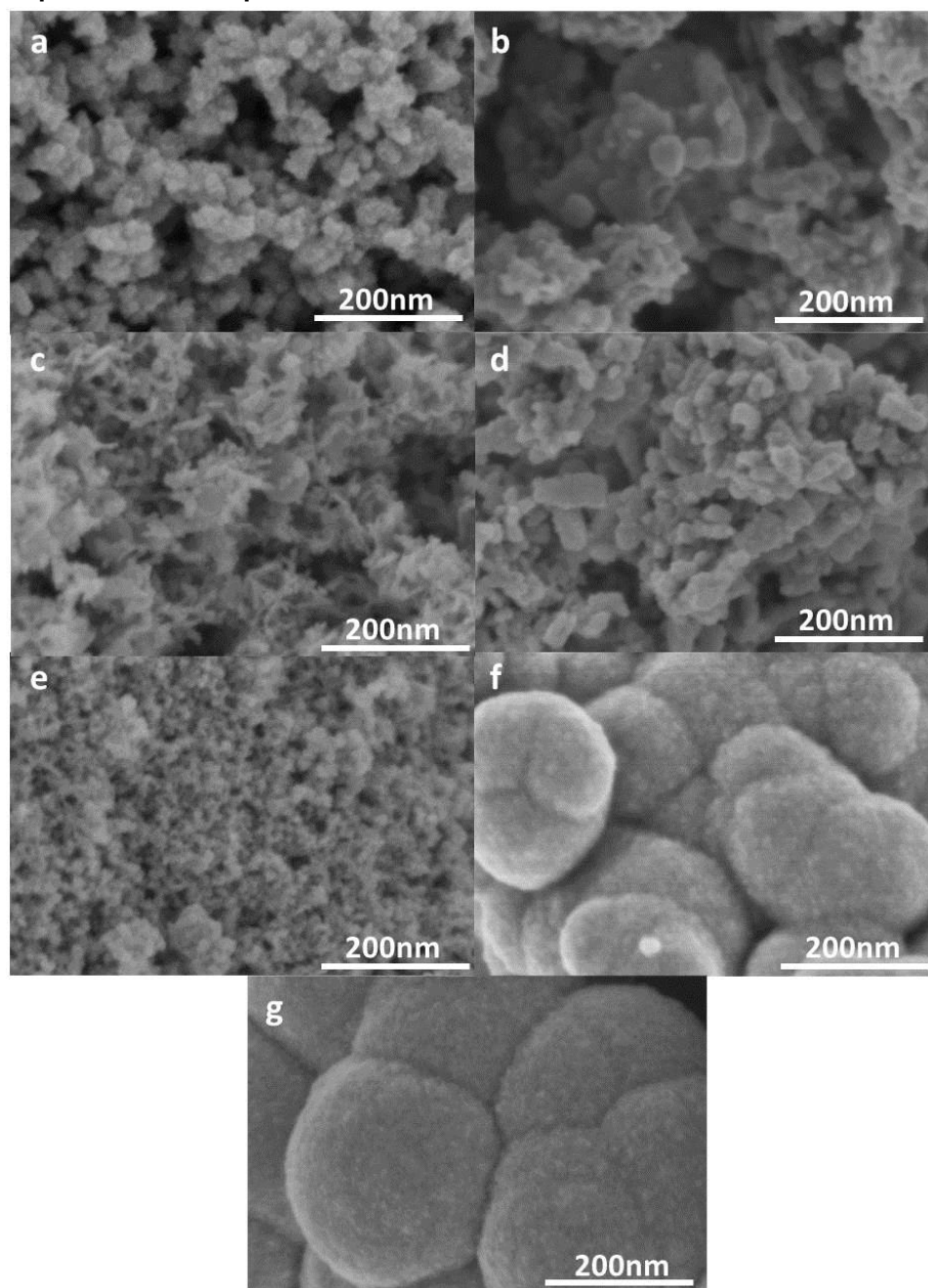


Figure S4. SEM-pictures (1.5KV) of the MW-produced Ir-compounds with initial KOH:Ir-ratios of 1:1 (a), 4:1 (b), 5:1 (c), 7:1 (d), 10:1 (e), 50:1 (f), 100:1 (g).

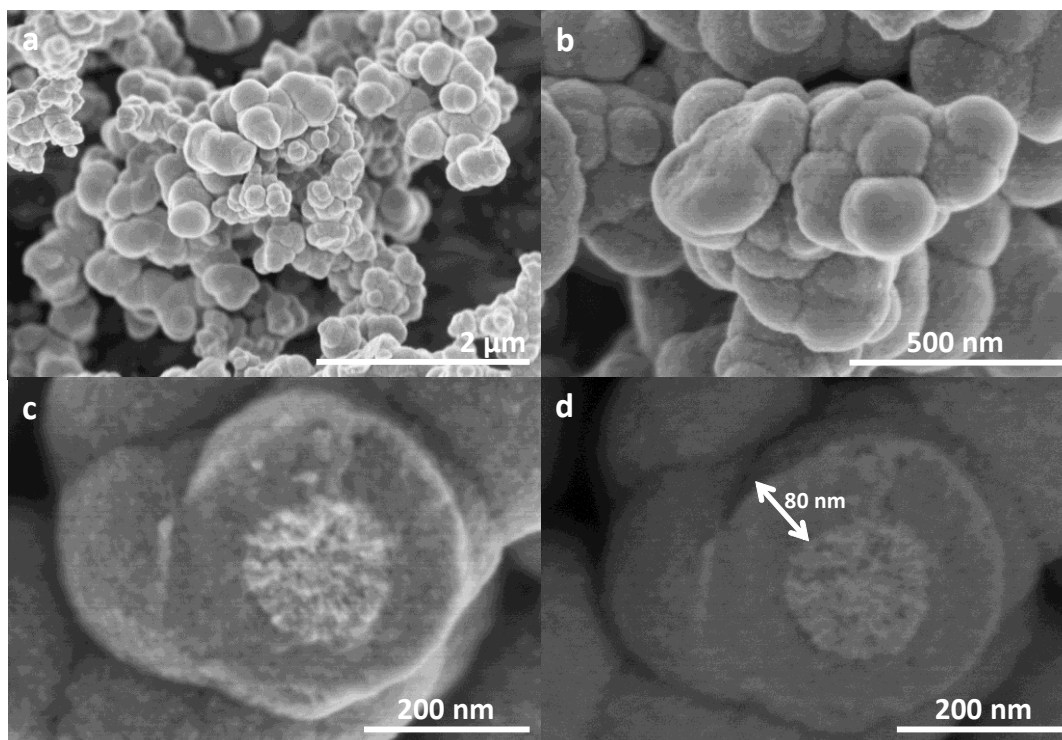


Figure S5. SEM-imagery of the Ir-compound produced for KOH:Ir=50:1 revealing spheric clusters (a,b). Analysis of split spheres (c) using a low-angle detector for atomic number sensitive secondary electron contrasted imagery (d) reveals a core-shell structure wherein a bright Ir-core is coated in a darker thick Ir-layer.

STEM-imaging

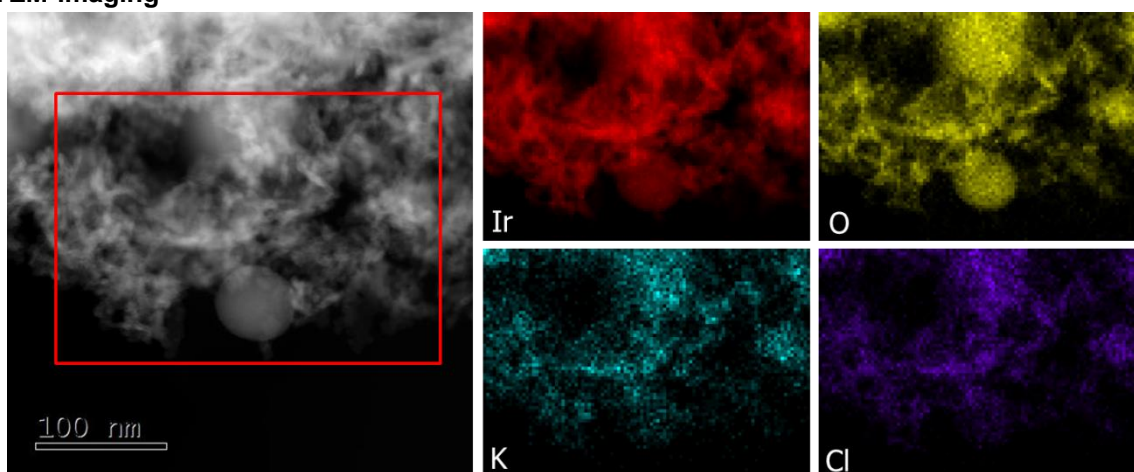


Figure S6. STEM-imaging of the Ir-compound obtained for KOH:Ir=5:1 and the corresponding EDX-mapping of Ir, O, K and Cl.

Thermogravimetric analysis (TGA) and Differential scanning calorimetry (DSC)

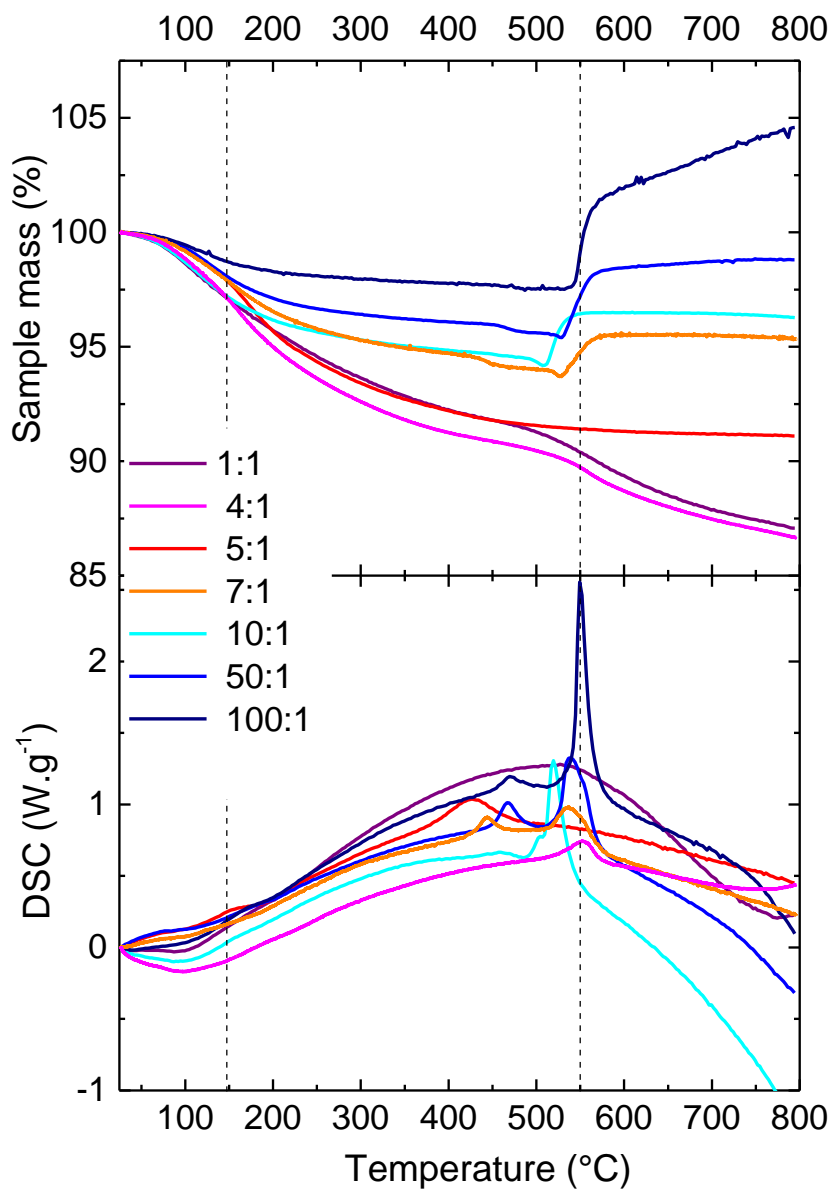


Figure S7. Thermogravimetric analysis (TGA) and differential scanning calorimetry (DSC) of Ir-based catalysts synthesized at several KOH:Ir ratios (see legend) under 100 mL min⁻¹ 21%O₂/Ar, 10 K min⁻¹

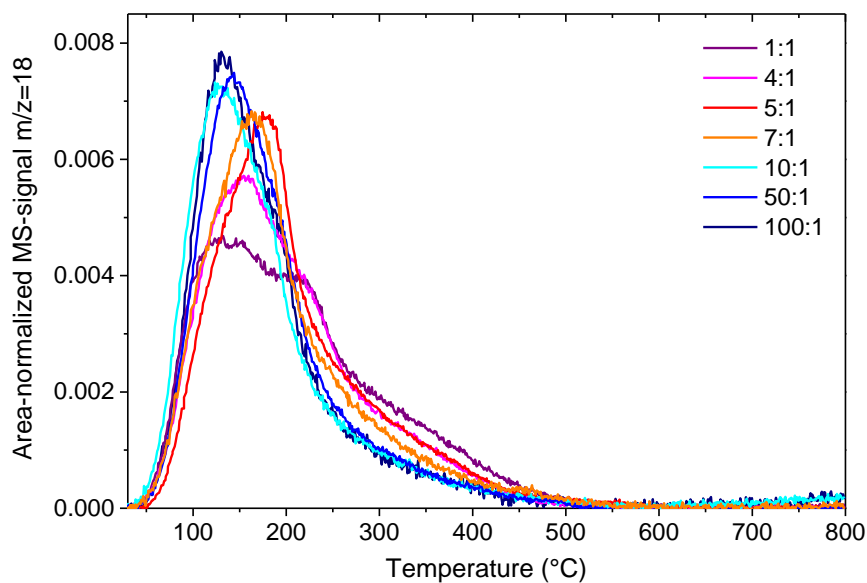


Figure S8. Area normalized mass spectrometry (MS) signal at $m/z=18$ during thermogravimetric analysis (TGA) of Ir-based catalysts synthesized at several KOH:Ir ratios, see legend.

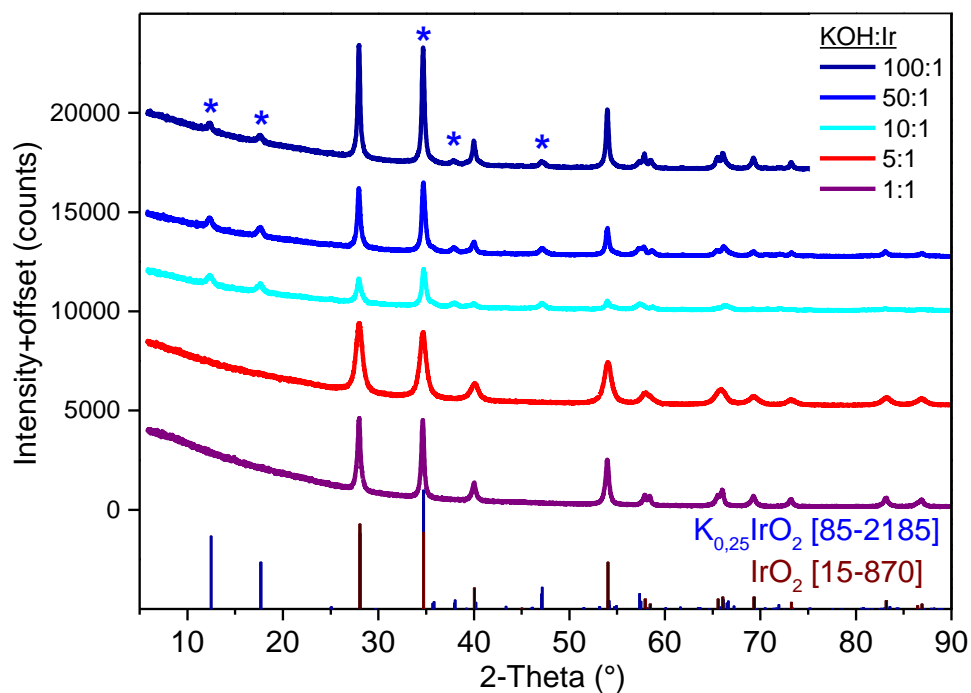


Figure S9. XRD of Ir-compounds after being subjected to the TGA-MS experiment where they were heated to 800°C in a 21%-O₂/Ar-flow (100 ml min⁻¹). The patterns support the complete oxidation of the samples to IrO₂ and hollandite K_{0.25}IrO₂.

Temperature programmed reduction (TPR)

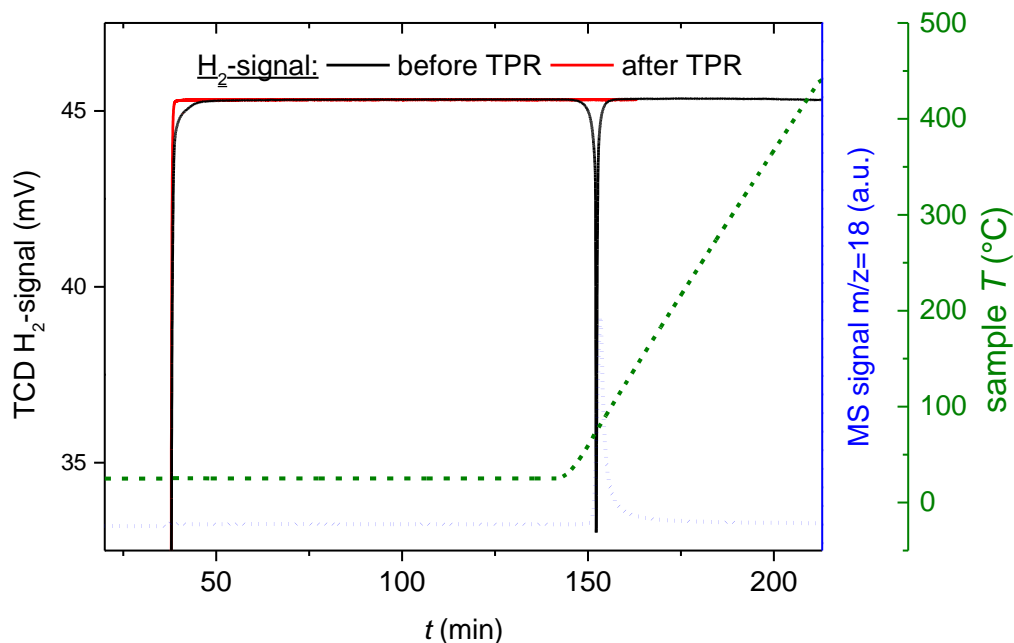
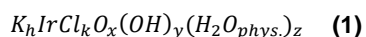


Figure S10. H₂-signals observed for the sample synthesized with a KOH:Ir ratio of 5:1 before (black line) and after TPR (red line). The discrepancy observed between the two signals during the switch from He to 5% H₂/He reveals an initial consumption of H₂ at RT without concomitant evolution of H₂O.

Quantification of the samples composition and average Ir-oxidation state

In order to determine sample composition and average Ir-oxidation state of the compounds, the nominal composition and molar mass of the compounds need to be determined. Taking into account all possible contaminants from initial reactants, the formula is:



- The average oxidation state of iridium is $1 + 2x + y$. The formula of each sample must thus be elucidated in order to assess its average oxidation state.
- The molar mass of the compound is given by :

$$M = M_K \times h + M_{Cl} \times k + M_{Ir} + M_O \times x + M_{OH} \times y + M_{H_2O} \times z \quad (2)$$

- K/Ir-, and Cl/Ir-ratios (h,k) were determined easily from XRF (see Table S1)
- TGMS gives access to the amount of physisorbed ($n_{H_2O}^p$) and chemisorbed ($n_{H_2O}^x$) water (two equations linking y and z) via the subsequent mass loss corresponding to the removal of first physisorbed water (mass fraction x_{m,H_2O}^p) and later chemisorbed water through hydroxyl decomposition (mass fraction x_{m,H_2O}^x).

Physisorbed water:

$$z \times n_{tot} = n_{H_2O}^{\phi} \Leftrightarrow z \times \frac{m_{tot}}{M} = \frac{m_{H_2O}^{\phi}}{18}$$

$$\mathbf{M \times x_{m,H_2O}^{\phi} = 18z \quad (3)}$$

Chemisorbed water:

$$(OH)_y = O_{y/2} + \frac{y}{2} H_2O$$

$$\frac{y}{2} \times n_{tot} = n_{H_2O}^{\chi} \Leftrightarrow \frac{y}{2} \times 18 = M \times x_{m,H_2O}^{\chi}$$

$$\mathbf{M \times x_{m,H_2O}^{\chi} = 9y \quad (4)}$$

- TPR yields a third equation linking x and y :

$$lCl + xO + yOH + \left(\frac{l}{2} + x + \frac{y}{2}\right)H_2 = lHCl + (x + y)H_2O$$

$$n_{H_2} = \left(\frac{l}{2} + x + \frac{y}{2}\right)n_{sample} = \left(\frac{l}{2} + x + \frac{y}{2}\right)\frac{m_{sample}}{M}$$

$$\mathbf{n_{H_2} \times M = \left(\frac{l}{2} + x + \frac{y}{2}\right)m_s \quad (5)}$$

Equations described above and highlighted in bold form a system of three linear equations in x,y and z, that was solved numerically using Wolfram Mathematica software. See Table S1 for the values of the the calculation parameters, i.e., $h, k, l, x_{m,H_2O}^{\phi}, x_{m,H_2O}^{\chi}, n_{H_2}$ and m_s for each synthesized compounds.

Additional information for the coefficients $x_{m,H_2O}^{\phi}, x_{m,H_2O}^{\chi}, n_{H_2}$ and x_{mol,Ir^0} :

- a) The mass fraction of physisorbed water x_{m,H_2O}^{ϕ} corresponds to the mass loss determined via TGMS between room temperature and, empirically defined 135°C which upper temperature corresponds to the maximum evolution rate of water
- b) The mass fraction of hydroxyl groups x_{m,H_2O}^{χ} corresponds to the mass loss determined between ca. 135°C and 500°C. The sample mass increase due to the oxidation of Ir³⁺ to Ir⁴⁺ was neglected, as well as, the mass loss due to the decomposition of surface carbonate and formate species
- c) The total H₂-consumption during TPR n_{H_2} takes into account the amount of hydrogen adsorbed at room temperature, as it also participated in the reduction of the sample.
- d) The mol.% of Ir⁰ x_{mol,Ir^0} was estimated from the sharp mass gain detected above 500°C for the samples synthesized with a KOH:Ir ratio of 7:1 to 50:1. This mass gain is associated with the oxidation of Ir⁰ to IrO₂ and the initial molar Ir⁰-content (x_{mol,Ir^0}) can be estimated as follows:

$$\%_{\text{mass gain, Ir}^0 \rightarrow \text{IrO}_2} = \frac{32 \times x_{mol,Ir^0}}{M_{ini}}$$

OER-activity evaluated from linear sweep voltammetry (LSV)

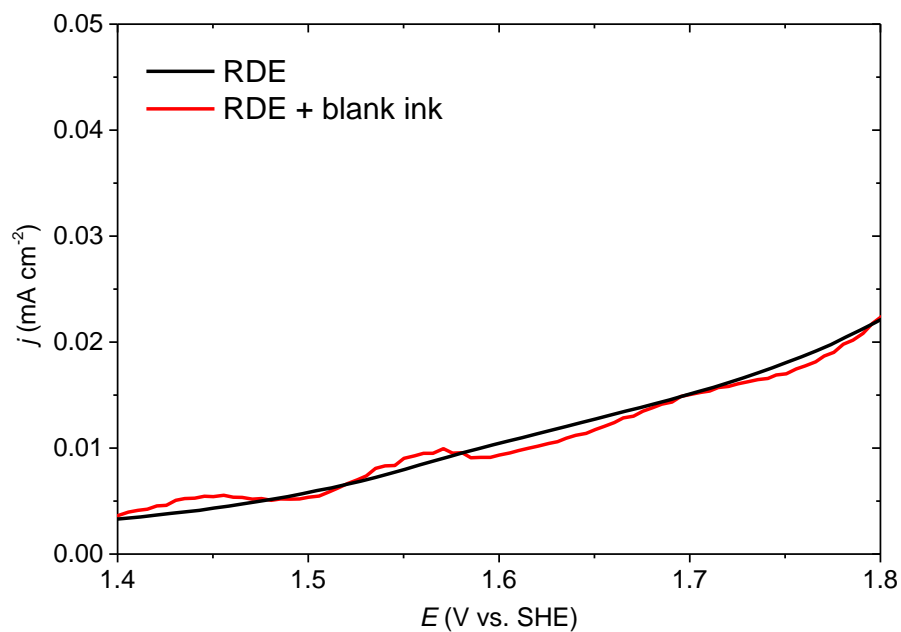


Figure S11. Linear sweep voltammograms of the pristine rotating disc electrode (black) and with blank ink on RDE (red).

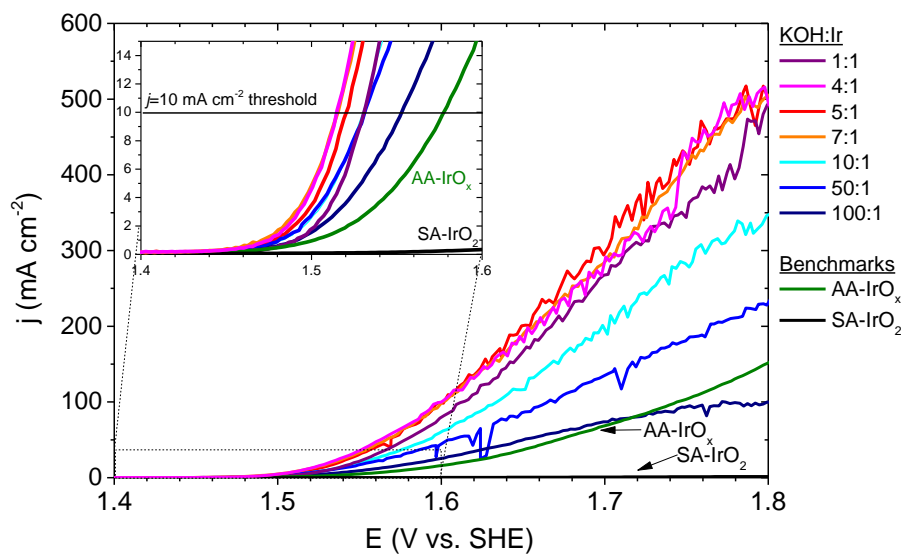


Figure S12. Linear sweep voltammograms of Ir-based catalyst synthesized with various KOH:Ir ratios, see legend, at 250°C for 1h and compared to amorphous (red) and crystalline (black) benchmark catalysts (dashed line).

OER-stability evaluated from chronopotentiometry (CP)

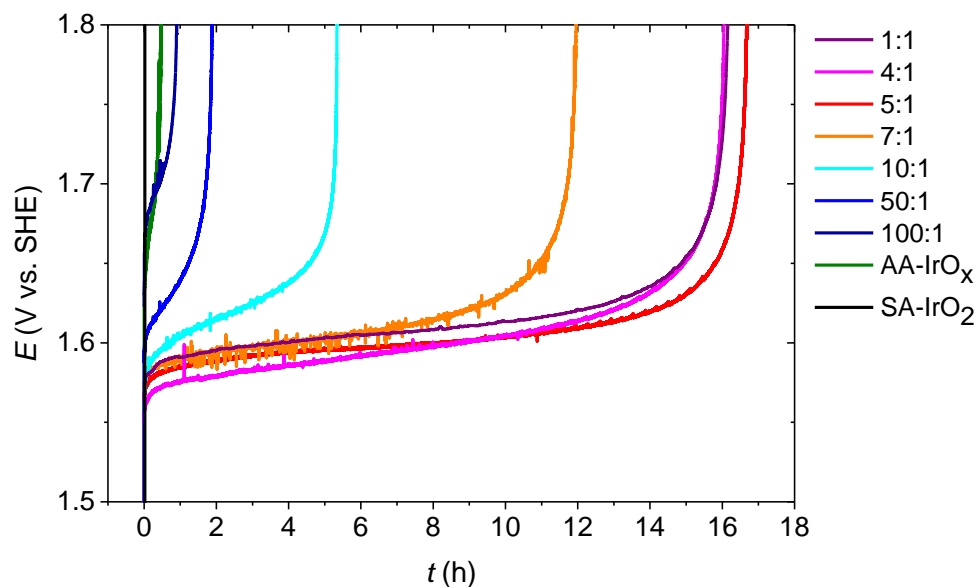


Figure S13. Chronopotentiometry at 15 mA cm^{-2} of Ir-based catalyst synthesized with various KOH:Ir ratios, see legend, at 250°C for 1h and compared to amorphous (red) and crystalline (black) benchmark catalysts (dashed line). The catalyst stability is defined as the time necessary to reach 1.8V which value corresponds to the onset of the glassy carbon electrode corrosion.

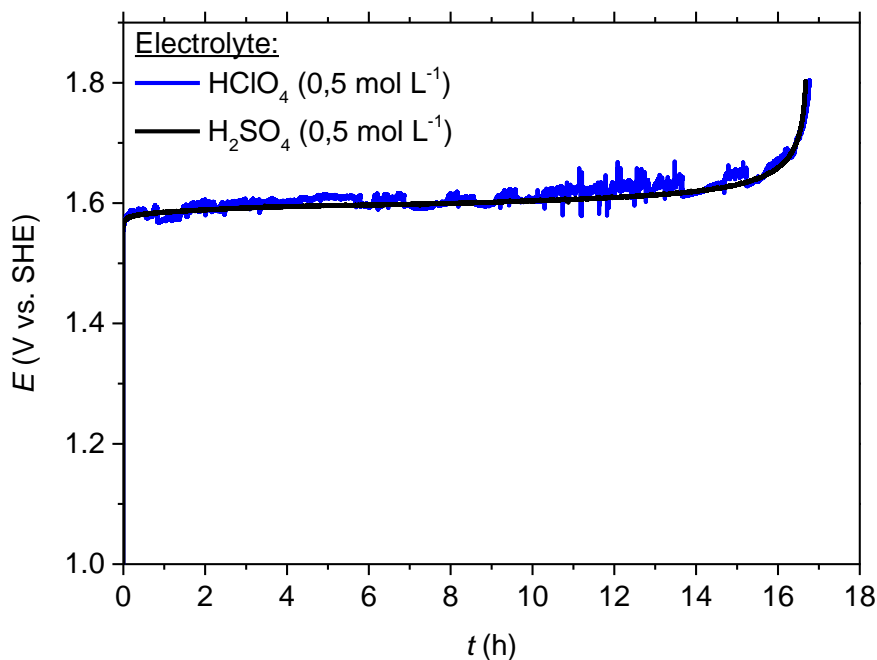


Figure S14. CP at $j=15 \text{ mA cm}^{-2}$ evaluated in H_2SO_4 and HClO_4 electrolytes for the Ir-oxohydroxide prepared from KOH:Ir=5:1.

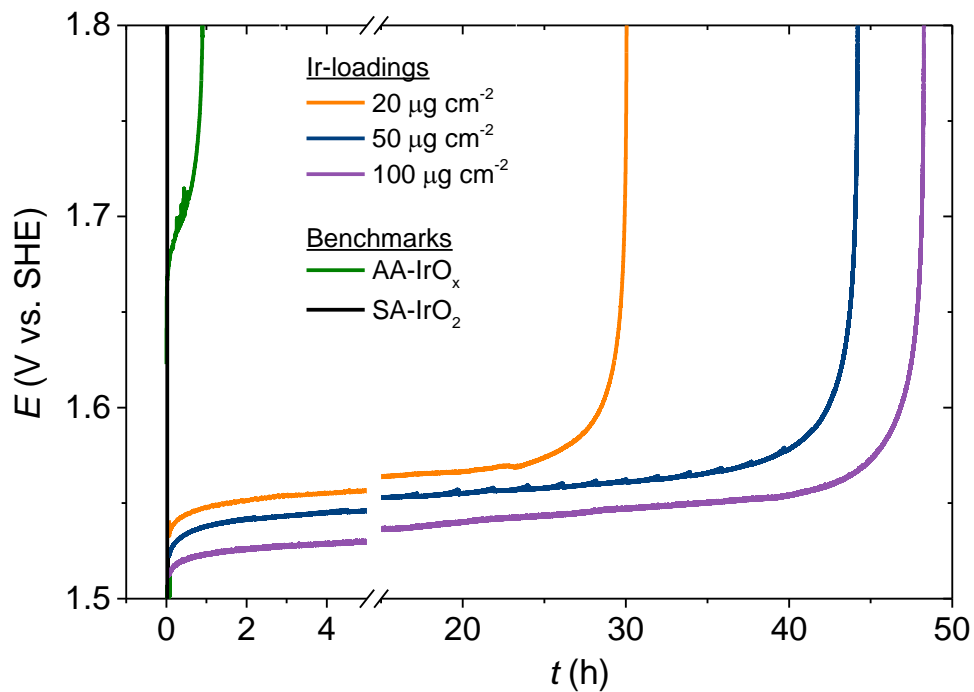


Figure S15. Chronopotentiometry at 10 mA cm⁻² for Ir-based catalyst synthesized using KOH:Ir=5:1 for electrode-loadings of 20, 50 and 100 $\mu\text{g}_{\text{Ir}} \text{cm}^{-2}$, (see legend), and compared to amorphous AA-IrO_x (green line) and crystalline SA-IrO₂ (black line) benchmark catalysts loaded at 20 $\mu\text{g}_{\text{Ir}} \text{cm}^{-2}$.